

NAVAL AIR WARFARE CENTER
TRAINING SYSTEMS DIVISION
ORLANDO, FLORIDA



TECHNICAL REPORT 95-003

**DETERMINING THE GAMMA OF
A NIGHT VISION DEVICE**

AUGUST 1997

CENTER OF EXCELLENCE
FOR SIMULATION AND
TRAINING TECHNOLOGY



NAWC

Training Systems Division

NAVAL AIR WARFARE CENTER

UNCLASSIFIED STATEMENT

For public release
Distribution Unlimited

TECHNICAL REPORT 95-003

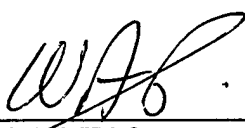
**DETERMINING THE GAMMA OF
A NIGHT VISION DEVICE**

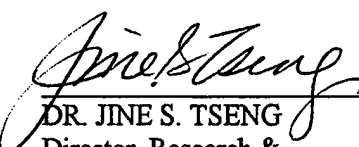
AUGUST 1997

John H. Allen
Richard C. Hebb

NAVAL AIR WARFARE CENTER
TRAINING SYSTEMS DIVISION
ORLANDO, FL 32826-3224

Approved for public release;
distribution is unlimited


W. A. RIZZO
Head, Science &
Technology Division


DR. JINE S. TSENG
Director, Research &
Engineering Department


W. T. HARRIS
Director, Research &
Technology

19970903 111

DTIC QUALITY INSPECTED

GOVERNMENT RIGHTS IN DATA STATEMENT

Reproduction of this publication in whole or in part is permitted for any purpose of the United States Government

REPORT DOCUMENTATION PAGE

1a. REPORT SECURITY CLASSIFICATION Unclassified			1b. RESTRICTIVE MARKINGS None		
2a. SECURITY CLASSIFICATION AUTHORITY			3. DISTRIBUTION / AVAILABILITY OF REPORT Approved for public release; Distribution is unlimited.		
2b. DECLASSIFICATION / DOWNGRADING SCHEDULE					
4. PERFORMING ORGANIZATION REPORT NUMBER(S) TECHNICAL REPORT 95-003			5. MONITORING ORGANIZATION REPORT NUMBER(S)		
6a. NAME OF PERFORMING ORGANIZATION Naval Air Warfare Center Training Systems Division		6b. OFFICE SYMBOL (If applicable) Code 4962		7a. NAME OF MONITORING ORGANIZATION	
6c. ADDRESS (City, State, and ZIP Code) 12350 Research Parkway Orlando, FL 32826-3224			7b. ADDRESS (City, State, and ZIP Code)		
8a. NAME OF FUNDING / SPONSORING ORGANIZATION Office of Naval Research		8b. OFFICE SYMBOL (If applicable) Code 342		9. PROCUREMENT INSTRUMENT IDENTIFICATION NUMBER	
8c. ADDRESS (City, State, and ZIP Code) 800 N. Quincy St. Arlington, VA 22217-5000			10. SOURCE OF FUNDING NUMBERS		
			PROGRAM ELEMENT NO. PE0602233N	PROJECT NO. RM33T24	TASK NO. 4761
11. TITLE (Include Security Classification) DETERMINING THE GAMMA OF A NIGHT VISION DEVICE (U)					
12. PERSONAL AUTHOR(S) Allen, John H. and Hebb, Richard C.					
13a. TYPE OF REPORT Interim		13b. TIME COVERED FROM JUN 94 TO NOV 94		14. DATE OF REPORT (Year, Month, Day) 1997, August, 19	
15. PAGE COUNT 34					
16. SUPPLEMENTARY NOTATION					
17. COSATI CODES			18. SUBJECT TERMS (Continue on reverse if necessary and identify by block number)		
FIELD	GROUP	SUB-GROUP	Night Vision Device, NVD, Night Vision Goggles, NVG, ANVIS, Simulation, Stimulation, Gamma, Night Spectra, Near IR, Spectral Response, Lambertian, Test Target, Gray Scale, NVIS, Radiance, Irradiance, Contrast, Response		
19. ABSTRACT (Continue on reverse if necessary and identify by block number) <p>The purpose of this report is to document a series of laboratory investigations and measurements beginning June 1994, relating to the imaging characteristics of a third generation Night Vision Device (NVD) operating under various input conditions. It also relates this information to environmental conditions encountered and subsequently recorded during preliminary field experiments.</p> <p>During data collection, a specially designed nine-patch gray scale target was evenly illuminated by a source. A third generation night vision monocular, with operational characteristics similar to that of the ANVIS, was aligned on an optical bench and focused onto the target. A photometer was used to measure the monocular target image at the fiber-optic bundle output. The irradiant energy directed at the target by the source was varied which, in turn, varied the average photocathode incident energy. At each change in irradiance, photopic measurements were made of the gray scale patch image displayed on the monocular output. By examining the relative luminance of the patches at the output and comparing it to the input NVIS radiance of the patches, the gamma of the NVD was determined.</p> <p>The data indicate that imagery produced by this particular NVD monocular will have a gamma close to unity.</p>					
20. DISTRIBUTION/AVAILABILITY OF ABSTRACT <input type="checkbox"/> UNCLASSIFIED/UNLIMITED <input checked="" type="checkbox"/> SAME AS RPT. <input type="checkbox"/> DTIC USERS			21. ABSTRACT SECURITY CLASSIFICATION Unclassified		
22a. NAME OF RESPONSIBLE INDIVIDUAL John H. Allen			22b. TELEPHONE (Include Area Code) (407)-380-4579		22c. OFFICE SYMBOL NAWCTSD 4962

THIS PAGE INTENTIONALLY LEFT BLANK

TECHNICAL REPORT 95-003

EXECUTIVE SUMMARY

INTRODUCTION

One of the research objectives of the Simulation of Advanced Sensors project is to display high fidelity night vision imagery captured under known environmental conditions. To meet this objective, various image acquisition and display methodologies are being explored. The purpose of this report is to document a series of laboratory investigations and measurements beginning in June 1994, relating to the imaging characteristics of a third generation Night Vision Device (NVD) operating under various input conditions. It also relates this information to environmental conditions encountered and subsequently recorded during preliminary field experiments.

GAMMA

Gamma is a term commonly used to describe the transfer function of a Cathode Ray Tube (CRT) device such as a video monitor. CRT video monitors by nature exhibit a nonlinear relationship between the input video signal and display output luminance. A monitor's output brightness is proportional to its' video input raised to some power. Third generation NVDs exhibit a characteristic gamma as well.

THE SPECTRAL NATURE OF THE NIGHT SKY AND NATURAL OBJECTS

Derived from both natural and artificial sources, the quantity and spectral content of ambient night sky energy varies with time of night, moon angle, moon phase, weather, and geographic location. The energy available to stimulate an NVD is a function not only of the available ambient energy, but also of the spectral reflectance of objects within the NVD's field of view.

ANVIS SPECTRAL RESPONSE

In general, an NVD like the Aviator's Night Vision Imaging System, or "ANVIS," responds only to a small segment of the total energy spectrum. Due to the spectral sensitivity of the third generation image intensifier tube itself, and filters which are added to the front end optics, the ANVIS reacts primarily to energy in the near infrared region.

NVD GAMMA TESTS

During data collection a specially designed nine-patch gray scale target was evenly illuminated by a source. A Litton third generation night vision monocular with operational characteristics similar to that of the ANVIS was aligned on an optical bench and focused onto the target. A calibrated Spectra Pritchard 1980A photometer was used to measure the monocular target image at the fiber-optic bundle output. The irradiant energy directed at the target by the source was varied which, in turn, varied the average photocathode incident energy. At each change in irradiance, photopic measurements were made of the gray scale patch image displayed on the monocular output. By examining the relative luminance of the patches at the output and comparing it to the input radiance of the patches, the gamma of the NVD was determined.

OBSERVATIONS AND CONCLUSIONS

Within the ability of the instruments to measure and/or the measurement procedures used, the data indicate that the imagery produced by this NVD monocular will have a gamma close to unity (1). Our measurements and data indicate that this particular NVD is linear over a wide range of input levels. Although an ANVIS was not used to obtain the data in this report, the observed findings should be applicable since the NVD monocular used for data gathering has the same image intensification tube and similar electronics. This does not imply that the operational characteristics of the two systems are identical, just that they are comparable.

THIS PAGE INTENTIONALLY LEFT BLANK

TECHNICAL REPORT 95-003

TABLE OF CONTENTS

	<u>Page</u>
INTRODUCTION	9
GAMMA	9
THE SPECTRAL NATURE OF THE NIGHT SKY	11
THE SPECTRAL NATURE OF NATURAL OBJECTS	12
ANVIS SPECTRAL RESPONSE	13
NVD GAMMA TESTS	14
EXPERIMENTAL OVERVIEW	14
GRAY SCALE TEST TARGET	15
IRRADIATING SOURCE MEASUREMENT AND COMPENSATION	18
NORMALIZED NVIS "A" NVD INPUT	19
NVD BUNDLE OUTPUT COMPENSATION	20
NORMALIZED NVD OUTPUT	21
OBSERVATIONS	22
CONCLUSIONS	28
REFERENCES	31

LIST OF ILLUSTRATIONS

<u>Figure</u>		<u>Page</u>
1	A Gamma of 2.2 vs. 1.0	10
2	AN/VS-6 Gain/Saturation Curve	11
3	Florida Night Sky Spectral Scans	12
4	Reflectance Data for Bahia Grass versus a Sandy Road	13
5	NVIS "A" Normalized Response	13
6	Experimental Setup for Obtaining Laboratory Data	14
7	Fiber Optic Bundle Output	15
8	Gray Scale Test Target	16
9	Percent Reflectance Versus Wavelength for Gray Scale Material Samples	17
10	NVD Response, Source at 45 and 40 Volts	24
11	NVD Response, Source at 35 and 30 Volts	25
12	NVD Response, Source at 25 and 20 Volts	26
13	NVD Response, Source at 15 and 10 Volts	27

LIST OF TABLES

<u>Table</u>		<u>Page</u>
1	Night Sky Energy	12
2	Gray Scale Sample Reflectance	18
3	Relative Incident Energy Map	19
4	Normalized NVIS "A" NVD Input	20
5	Normalized NVD Bundle Output Map	20

THIS PAGE INTENTIONALLY LEFT BLANK

INTRODUCTION

Sensitive mainly to energy in the near infrared (IR) portion of the electro-magnetic spectrum, third generation, or "Gen 3" Night Vision Devices (NVDs) such as the AN/AVS(6) are now in common use by Navy and Marine Corps aviators. Although Gen 3 NVDs allow low altitude night operations to be conducted under diverse environmental conditions, the appearance of targets and terrain as viewed through an NVD are not constant. Imagery, dependent upon weather, moon-phase, moon-angle, and viewing direction, can be contrary to user expectations. Contrast of passive objects within the field of view depends upon each object's ability to reflect available near infrared energy and the NVD's ability to transform invisible near infrared energy into visible photopic energy.

One of the research objectives of the Simulation of Advanced Sensors project is to display high fidelity night vision imagery captured under known environmental conditions. To meet this objective, various image acquisition (Allen, Hebb (1993)) and display methodologies are currently being explored. Acquiring high quality NVD images and environmental data is not a straightforward process. Problems easily resolved under laboratory conditions become insurmountable in the field. Some data can be obtained only by the use of state of the art equipment. Many procedures are not standardized and are subject to gross errors, both in measurement and interpretation. Finally, proper display of the acquired imagery requires knowledge of the NVD's characteristic imaging response at the time of image acquisition.

Although data in MIL-I-49428 strongly indicate that the gain of the AN/AVS(6) Night Vision Goggle (NVG) system is linear, it was not known (by the authors) whether the system was indeed linear over its useful range of input energy conditions. From our own field observations and undocumented discussions with knowledgeable users, we first surmised that under low ambient energy (light) levels, that the NVG would begin to exhibit nonlinearity. Although the findings in this report do not support our original hypothesis, the observed linear behavior is an important consideration not only for NVG simulation and modeling but users as well.

The purpose of this report is to document a series of laboratory investigations and measurements beginning in June 1994, relating to the imaging characteristics of a Gen 3 NVD. Data regarding the linearity of the gain or "gamma" is provided for various input conditions. It also relates this information to environmental conditions encountered and subsequently recorded during preliminary field experiments. These data and findings are presented below.

GAMMA

Gamma is a useful term which is commonly used to describe the transfer function of a cathode ray tube (CRT) device such as a video monitor. CRT video monitors by nature exhibit a nonlinear relationship between the input video signal and display output luminance. The monitor output luminance or photometric brightness is proportional to the monitor video input raised to some

power. By design, video cameras compensate for monitor nonlinearity by introducing an opposing nonlinear image gain during image capture; the whole process then neatly resolves itself and is of little consequence to most casual observers. Proper compensation is not automatically provided by all image sources. But the monitor is an equal opportunity device. It applies the same nonlinear gain to all input.

This relationship between the input image and the displayed or output image can be expressed in it's simplest form as:

$$\text{IMAGE OUTPUT} = (\text{IMAGE INPUT})^{2.2}$$

In this instance the "Gamma" is 2.2, a typical value for most CRT monitors. Figure 1 graphically illustrates this relationship. To be displayed correctly on a CRT monitor, the input imagery must be "gamma corrected", or compensated in some manner.

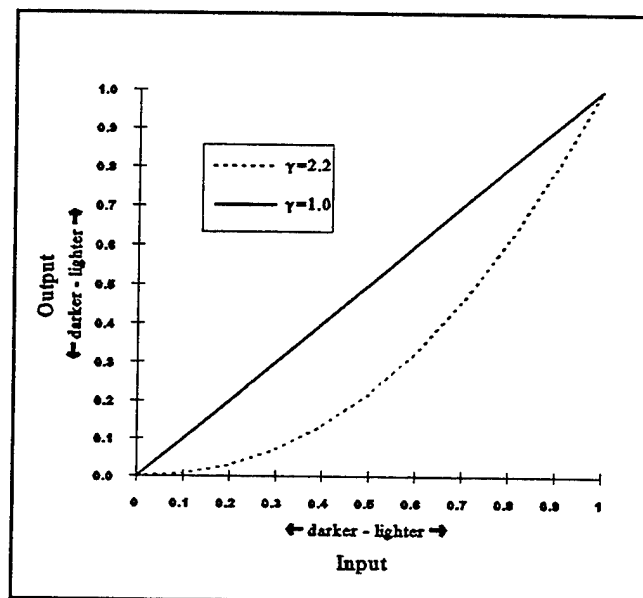


Figure 1. A Gamma of 2.2 vs. 1.0

An uncompensated black and white image will typically appear to be too dark. Objects within the scene which may be just visible in the real world will exhibit little or no contrast when displayed on the monitor and hence may not be visible at all. A properly compensated image, one whose correction "reverses" the effect of the monitor, will be neither too dark nor too light when it is viewed.

The image is "Gamma Corrected" or compensated by altering the relationship of its dark to light tones in a mathematically precise manner. For example, if a gamma compensation of $1/2.2$ is applied to the image before it is displayed, the effect of the monitor gamma of 2.2 is effectively canceled out:

$$\text{IMAGE OUTPUT} = (\text{IMAGE INPUT}^{1/2.2})^{2.2}$$

or:

$$\text{IMAGE OUTPUT} = \text{IMAGE INPUT}$$

In this very simplistic case objects within the original scene which are just visible in the real world will be just visible on the monitor assuming that the average luminance of the displayed image is close to the original. This is a basic description of gamma...at least as it is conventionally used. What is the gamma of a Gen 3 Night Vision Device (NVD)?

MIL-I-49428, the military specification for the Image Intensifier Assembly used in the AN/AVS-6(V), addresses luminance gain in paragraph 3.6.8. It does not, however, specifically address the linearity of the gain or gamma. Figure 6, Gain/Saturation Requirements, of the same military specification, reproduced here as Figure 2, does seem to indicate a linear relationship between

photocathode illumination and screen brightness at lower photocathode illumination levels. These curves, however, were generated under test conditions of even photocathode illumination and depict conditions under which Automatic Brightness Control (ABC) is in effect. It does not reveal how the system responds to real world input under those same ambient energy conditions.

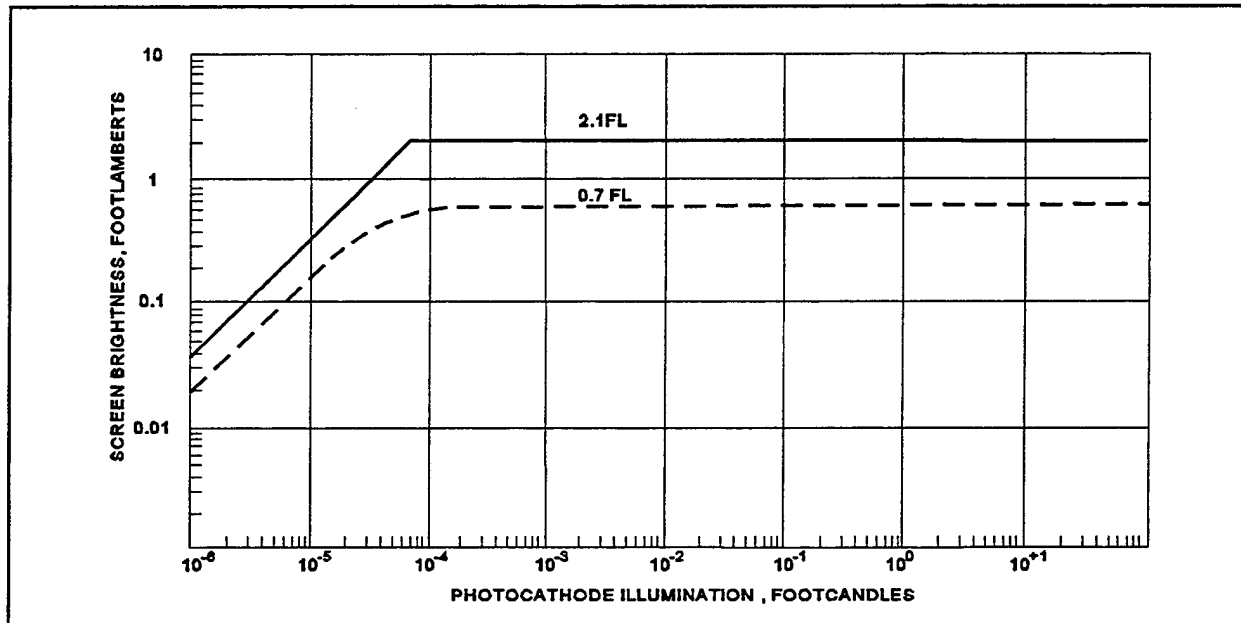


Figure 2. AN/AVS-6 Gain/Saturation Curve

THE SPECTRAL NATURE OF THE NIGHT SKY

Derived from both natural and artificial sources, the quantity and spectral content of ambient night sky energy varies with time of night, moon angle, moon phase, weather, and geographic location. Figure 3 shows a succession of night sky spectral scans that we obtained at a remote Florida location during a recent September moonlit night. Data collection was performed in a manner similar to that described by Stephanik (1989). The data have been smoothed somewhat to enhance graphing and interpretation. The vertical scale depicts irradiance in picowatts per centimeter squared per nanometer ($\text{pW}/\text{cm}^2\text{-nm.}$) The horizontal scale represents the wavelength in nanometers. Note how both the shape and height of the curves change with time. This particular data set demonstrates the effects of changing moon angle, and weather at a specific geographic location. The first three scans were taken early during the night and show the effects of cloud banks to the East and West reflecting distant city lights. As the weather clears, there is less cloud reflection, and the city lights' contribution to the overall nighttime illumination is less. Indications of this are seen mainly in the difference in curve shapes that occur between 540 and 660 nanometers over the six hour time span. Changes in the relative level of the curves demonstrate variation in available moonlight due to changing cloudcover and angular position of the moon above the horizon or moon angle. The accompanying data in Table 1 show the total available photopic energy both in footcandles and lux. The NVIS "A" radiance shown in the last column is calculated as described in paragraph 6.5.8 of military

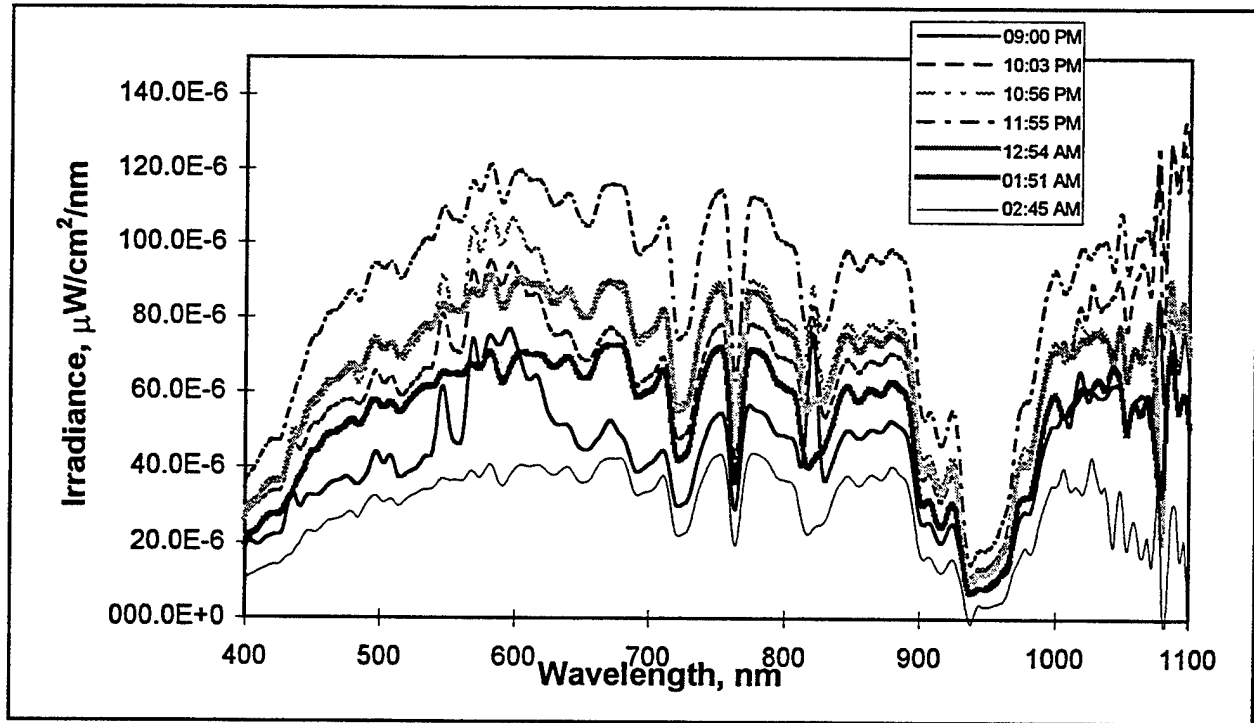


Figure 3. Florida Night Sky Spectral Scans

specification MIL-L-85762A and in this report is intended to be used as a relative measure of the total energy available to the AN/AVS-6 night vision goggles. Conditions in the night sky are certainly not static.

SCAN #	TIME OF NIGHT	ILLUMINANCE (fc)	ILLUMINANCE (lux)	NVIS "A" RADIANCE (NR _A)
1	2100	3.73e-03	4.02e-02	3.62e-09
2	2203	5.17e-03	5.57e-02	5.21e-09
3	2256	5.91e-03	6.36e-02	6.00e-09
4	2355	7.23e-03	7.79e-02	7.61e-09
5	0054	5.51e-03	5.93e-02	5.80e-09
6	0151	4.31e-03	4.64e-02	4.64e-09
7	0245	2.44e-03	2.62e-02	2.72e-09

Table 1. Night Sky Energy

THE SPECTRAL NATURE OF NATURAL OBJECTS

The energy available to stimulate the AN/AVS-6 night vision goggles or ANVIS (Aviator's Night Vision Imaging System) is a function not only of the quantity and spectral content of the available ambient energy, but also of the spectral reflectance of objects within the ANVIS field of view. Both natural and manmade materials absorb or reflect various wavelengths; we see a *red* object because it absorbs blue and green, but reflects red. Green plants appear *green* because they reflect

green. Oddly, green plants are also good near IR reflectors. So too are dry sandy roads. Measured at the same remote Florida site discussed above, Figure 4 shows the reflectance of a patch of green Bahia grass compared with the reflectance of a nearby patch of dry sandy road. Note the similarities and therefore lack of contrast between grass and road in the near IR portion of the spectrum. Under certain conditions, when viewed through the NVD, low contrast between the road and grass will cause the two to appear continuous and the road will seem to disappear.

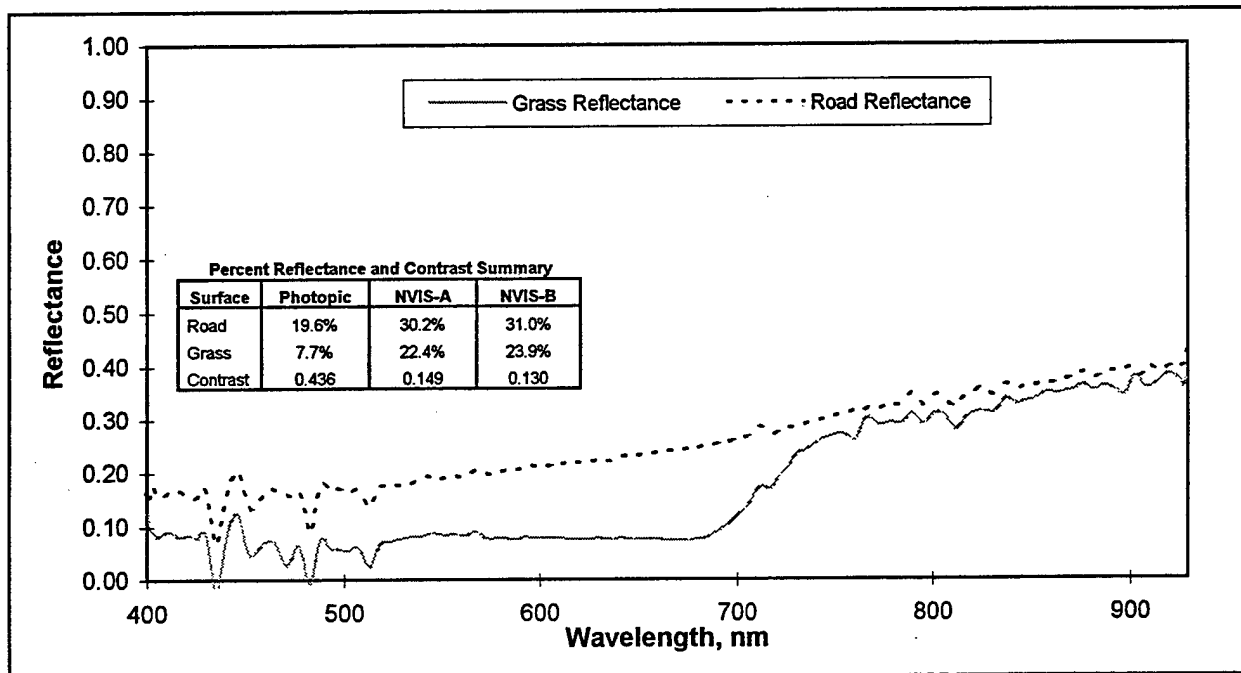


Figure 4. Reflectance Data for Bahia Grass versus a Sandy Road

ANVIS SPECTRAL RESPONSE

In general, the ANVIS responds only to a small segment of the total electro-magnetic spectrum. Due to the spectral sensitivity of the third generation (often referred to as Gen III) image intensifier tube itself, and filters which are added to the front end optics, the ANVIS reacts primarily to energy in the near IR region. It is relatively insensitive to blue and green light and somewhat sensitive to red. Figure 5 depicts the NVIS (Night Vision Imaging System) "A" response curve which is the relative spectral response of the NVIS using a 625nm "minus blue filter." The ANVIS meets the requirements of a Class A NVIS as defined by MIL-L-85762A, paragraph 6.5.1.3, however, the response curve may be different for an ANVIS with an additional light interference filter (LIF) installed.

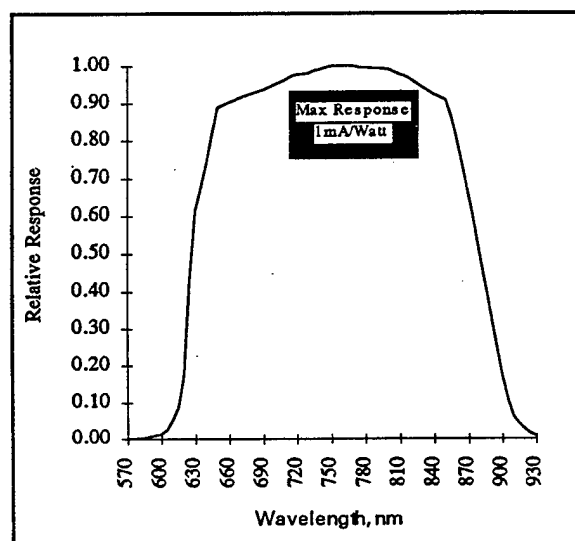


Figure 5. NVIS "A" Normalized Response

NVD GAMMA TESTS

Under real world conditions, the total energy that is useful to the ANVIS varies widely. It changes with nighttime ambient energy conditions, weather and also with the objects being viewed. In our laboratory tests, we attempted to mimic these dynamic conditions by viewing a specially designed gray scale target under a range of irradiance levels with a third generation NVD monocular.

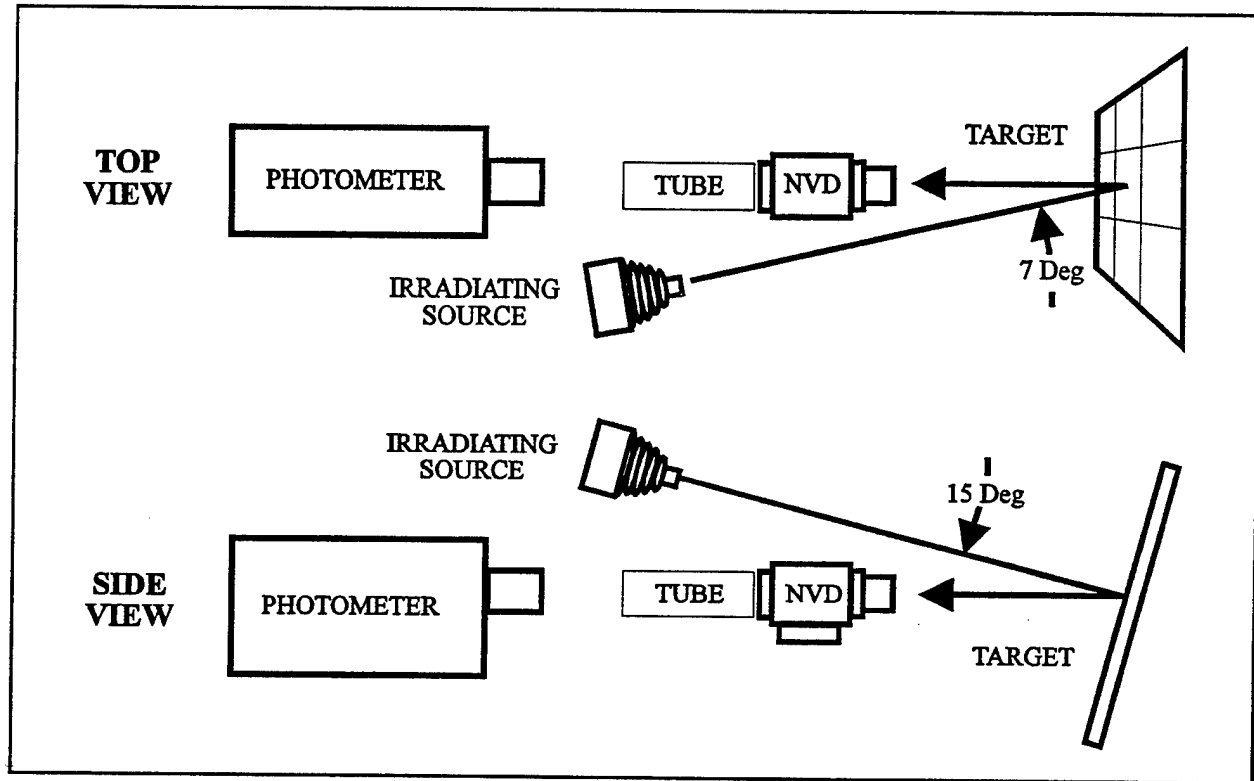


Figure 6. Experimental Setup for Obtaining Laboratory Data

EXPERIMENTAL OVERVIEW

Figure 6 shows the experimental setup used to determine NVD gamma. During the data collection, a specially designed nine-patch gray scale target, depicted in Figure 8, was evenly illuminated by a tungsten source. A Litton third generation night vision monocular, with operational characteristics similar to that of the ANVIS without a LIF filter, was aligned on an optical bench and focused onto the target. Corner to corner, the target occupied nearly the whole 40 degree NVD monocular field of view. The monocular eye piece was then removed. A calibrated Spectra Pritchard 1980A photometer was focused onto the fiber-optic bundle output of the monocular and arranged so that it could be directed at different areas of the fiber-optic bundle output shown in Figure 7. This allowed us to view and measure any portion of the target displayed at the output of the monocular. The irradiant energy directed at the target by the source was varied which, in turn, varied the average photocathode incident energy. At each change in irradiance, photopic measurements were made of the gray scale patch imagery displayed on the monocular output. By examining the relative luminance

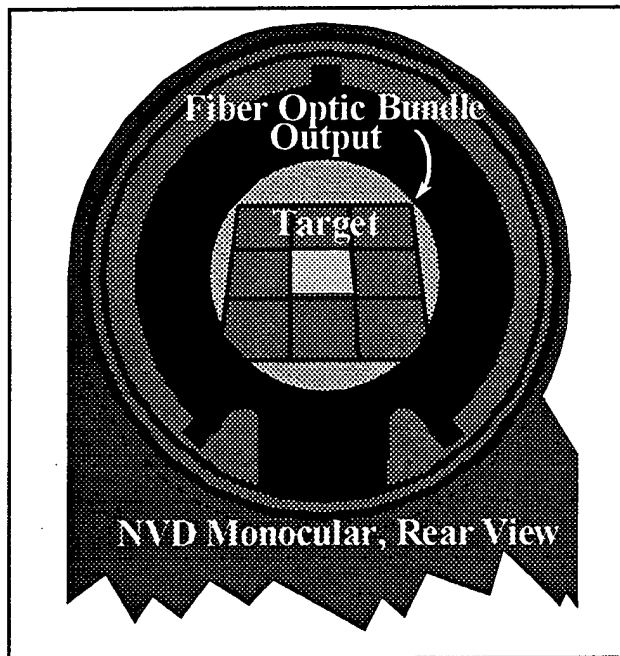


Figure 7. Fiber Optic Bundle Output

of the patches at the output and comparing it to the NVIS reflectance of the patches being input, the gamma of the NVD was determined.

After power up, the photometer was allowed to stabilize for two to three hours before use. During data acquisition, the irradiating source voltage was set to a value, laboratory lights secured, and the photometer focused. The photometer aperture was set to six minutes of arc for data acquisition from the NVD output and one degree of arc when data was acquired from the target.

A constant, even irradiance over the ANVIS photocathode does not result in even output luminance across the fiber bundle output face. Its profile varies, with the center region of the circular face being brighter than the edges. This effect is referred to in MIL-I-49428, paragraph 4.6.13, as output brightness

nonuniformity. We devised tests to determine and thereby separate the effects of output brightness nonuniformity from the data gathered to determine gamma.

Referring back to Figure 6, the NVD monocular and photometer were optically aligned along an axis striking the center of the gray scale test target. To avoid shadowing, the irradiant source was directed towards the target at a horizontal angle of approximately seven degrees from the optical axis. The target was tilted up by fifteen degrees and the source was tilted downward by the same amount in an attempt to even the irradiance across the target as much as possible. A regulated voltage source provided power to the irradiant source and allowed the amount of energy striking the target to be controlled.

GRAY SCALE TEST TARGET

The gray scale target used in these experiments was composed of a special purpose gray scale material normally used to electronically measure the response of video cameras. Although the percent reflectance of the material was photopically specified, it was not calibrated for near IR use. As previously demonstrated by the graphs in Figure 4, it is dangerous to assume that the reflectance of an object remains constant with changing wavelength. This was also true of the gray scale material used to form the nine patches in the target.

For this material to be useful, its spectral reflectance throughout the photopic and near IR wavelengths had to be determined. The procedure was as follows: First a uniformly radiating tungsten source was directed at a calibrated 18 inch square lambertian surface. Then, using a spectroradiometer, energy reflected from the lambertian surface at wavelengths between 400 and

1100 nanometers was measured. Next, a 12 inch square sample of the gray scale material was substituted for the lambertain reference and similar measurements made. This process was repeated for each material sample.

The lambertian reference surface was supplied from the manufacturer with a reflectance calibration, $L_r(\lambda)$. Using the energy reflected off the lambertian surface (lying in the same plane and position as the samples) as a reference allowed us to transform the reflected energy data obtained from the material samples into percent reflectance as a function of wavelength. This was accomplished by first multiplying the energy reflected from the reference, $L_r(\lambda)$, by the inverse of the reference reflectance calibration, $L_c(\lambda)$, to obtain a reference measure of the incident energy, $E_i(\lambda)$, or:

$$L_r(\lambda) * 1 / L_c(\lambda) = \text{Incident Energy, or } E_i(\lambda).$$

$E_i(\lambda)$ represents the energy incident on the reference surface as a function of wavelength prior to any reflection or absorption by the material samples. Next, the energy reflected by each gray scale sample, $S_r(\lambda)$, was divided by the incident energy, $E_i(\lambda)$, to get:

$$S_r(\lambda) / E_i(\lambda) = \text{Normalized Sample Reflectance, or } S(\lambda).$$

Multiplication by 100% produces the percent reflectance as a function of wavelength for each of the material samples. A graph of the percent reflectance versus wavelength extending from 400 to 1100 nm for each of the nine gray scale material samples is shown in Figure 9.

The photopic reflectance of each of the gray scale material samples was determined by first taking each of the normalized sample reflectance curves, $S(\lambda)$, multiplying them by the normalized CIE response curve, $K(\lambda)$, and integrating the result from 380 to 780nm. The reflectance is then obtained by dividing by the integral of the CIE curve as shown in the general equation below:

$$\text{Photopic Sample Reflectance} = \frac{\int_{380}^{780} S(\lambda) K(\lambda) d\lambda}{\int_{380}^{780} K(\lambda) d\lambda} \times 100\%.$$

The result of this operation for each of the nine material samples is listed in Table 2, Column 1 under the heading "Photopic Reflectance (%)."

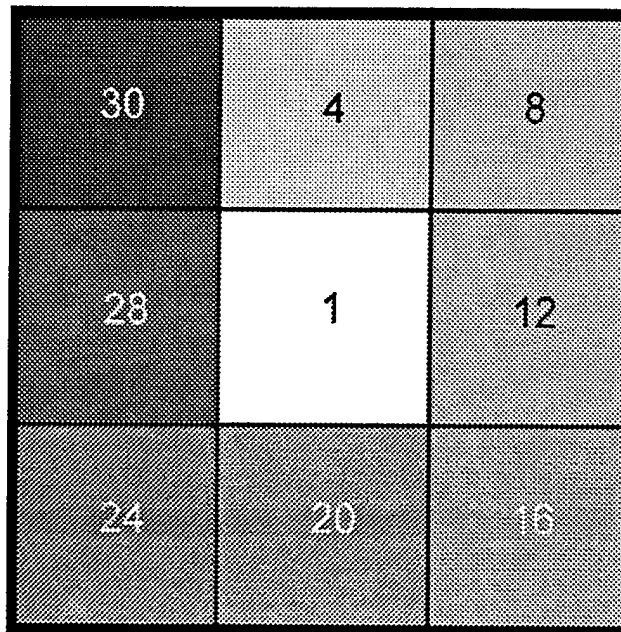


Figure 8. Gray Scale Test Target

Determination of the NVIS reflectance required a similar set of operations. Each normalized reflectance data curve ($S(\lambda)$) was multiplied by the NVIS "A" response curve, $G_A(\lambda)$, seen in Figure 5, and the result integrated from 530 to 930 nm. The results of this operation were then divided by the integral of the NVIS "A" response to give the NVIS "A" reflectance in percent. The operation is represented by the following general equation:

$$\text{NVIS "A" Reflectance} = \frac{\int_{530}^{930} S(\lambda) G_A(\lambda) d\lambda}{\int_{530}^{930} G_A(\lambda) d\lambda} \times 100\%.$$

These results are listed in Table 2, Column 3 for each of the nine material samples under the heading "NVIS 'A' Reflectance (%)." Column 4 of this table lists these gray scale sample reflectances with a normalization relative to sample #1.

In general, photopic reflectance varies from NVIS "A" reflectance for each sample. Some instances are more profound than others. Photopic and NVIS "A" reflectance differences depend entirely on the relative spectral reflectances across the photopic and NVIS "A" wavelength ranges.

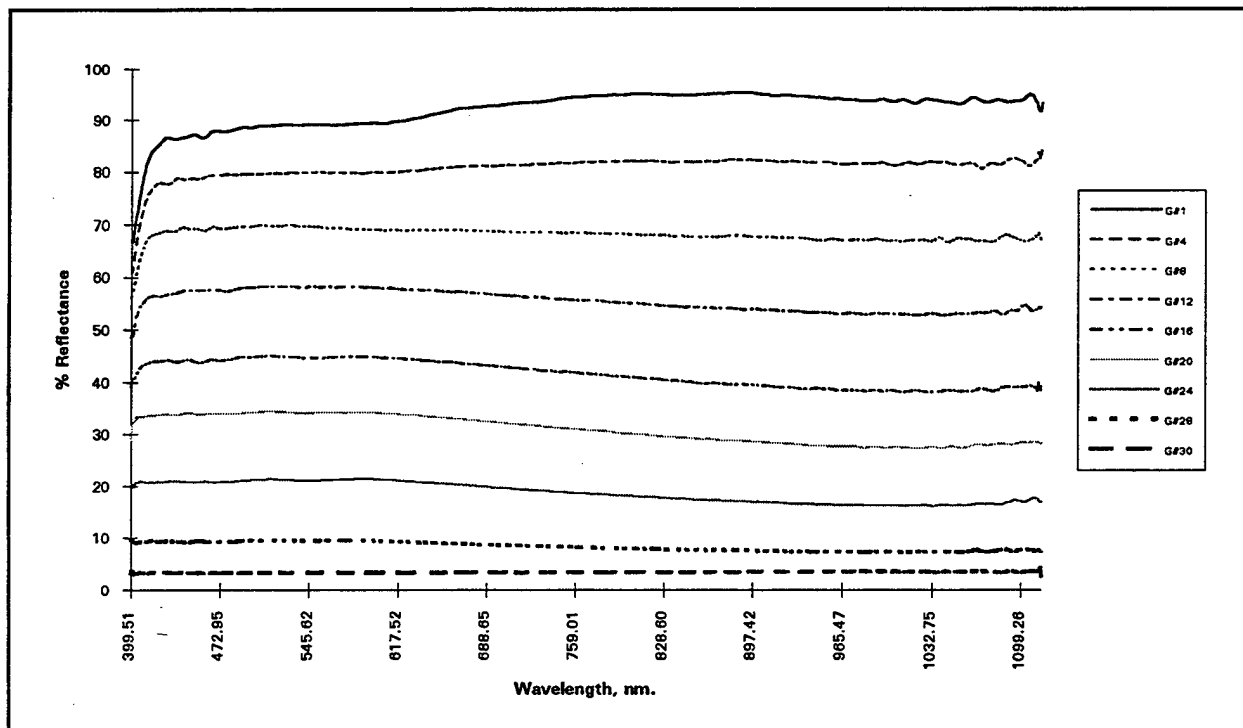


Figure 9. Percent Reflectance Versus Wavelength for Gray Scale Material Samples

Since the "gray" samples do not have identical uniform "flat" spectral reflectances, the characteristic NVIS "A" radiance of each sample does depend on the spectral nature of the irradiating source. So, irradiating sources having substantially different spectral profiles may result in slightly different NVIS contrasts. Energy reflected by the target at any single wavelength is a function of

the incident power at that wavelength and the sample reflectance at that same wavelength. The slight differences in the shape (slope) of the reflectance curves of the samples, as observed in Figure 9, did make the NVIS radiance of each sample somewhat susceptible to changes in the spectrum of the

GRAY SCALE SAMPLE #	PHOTOPIC REFLECTANCE (%)	NVIS "A" REFLECTANCE (%)	NORMALIZED NVIS "A" REFLECTANCE RELATIVE TO SAMPLE #1
1	89.19	93.81	1.000
4	79.82	81.48	0.869
8	69.38	68.38	0.729
12	58.04	55.75	0.594
16	44.67	41.85	0.446
20	34.08	31.07	0.331
24	21.18	18.83	0.201
28	9.43	8.26	0.088
30	3.31	3.39	0.036

Table 2. Gray Scale Sample Reflectance

irradiating source. Although the spectrum of the irradiating source used in this experiment did change slightly with voltage, we assumed that the *normalized* NVIS "A" radiance of each sample was constant and essentially equivalent to it's normalized NVIS "A" reflectance shown in Table 2.

IRRADIATING SOURCE MEASUREMENT AND COMPENSATION

NVIS "A" radiance was measured at each source voltage setting using a spectroradiometer and a calibrated lambertian surface located in the same position and distance as the gray scale target. The lambertian surface filled the field of view of the spectroradiometer. Although this measurement was useful for purposes of comparison to night sky data, it represented an *average* value across a large irregular area that was not necessarily coincident with that of the gray scale target. For this reason, this data could not be used to determine NVD gamma nor could this approach be used to determine the uniformity of the target surface irradiance.

Since precision measurement of small localized areas could not be made with the spectroradiometer we used another technique.

To determine the distribution of the source irradiance across the plane of the gray scale target surface, and to map out any non-uniformity effects, *photopic* measurements were made across the same lambertian surface. The assumption was that the photopic energy distribution would or should be consistent with the near IR energy distribution. These measurements were made at the intended center of each gray sample square of the gray scale target. The measurements were performed by removing the gray scale target, and substituting the lambertian surface overlaid with an open wire grid whose dimensions were identical to the sample squares' size and location. The wire grid served to

locate the gray scale sample boundaries, allowing the lambertian surface to be measured relative to the sample square locations. During these distribution measurements, the irradiating source was set to 40 volts (enough illumination to clearly see the wire grid) and the laboratory lights secured. This same procedure was also initially used in setting up both source and target in order to obtain as even an irradiance as possible. A further assumption was that the spatial uniformity of the irradiating source was invariant with change in voltage.

GRAY SCALE SAMPLE AREA #	AREA LUMINANCE (ft-L)	RELATIVE INCIDENT ENERGY
1	10.45 E-4	1.000
4	10.31 E-4	0.987
8	10.39 E-4	0.994
12	10.54 E-4	1.009
16	10.65 E-4	1.019
20	10.56 E-4	1.011
24	10.24 E-4	0.980
28	10.25 E-4	0.981
30	10.08 E-4	0.965

Table 3. Relative Incident Energy Map

Photopic measurements in foot-Lamberts (ft-L) were made at the centroid of each of the nine squares defined by the wire grids. The raw data in foot-Lamberts is given in Table 3, column 2. Column 3 contains the data from column 2 referenced to sample area #1. Sample locations on the gray scale test target are numbered as shown previously in Figure 8 starting with #1 in the center, #4 at the top center, #8 at the top right, and so on. Two pieces of data were recorded for sample location #1. It was always measured twice, at the start and at the finish. This served as a convincing evidence for or against any photometer or irradiating source drift. The average of the two data values for sample location #1 is used as the 100 percent reference. We refer to the center referenced luminance variation seen in Table 3 as the "Relative Incident Energy Map."

NORMALIZED NVIS "A" NVD INPUT

The relative incident energy map is used to determine the normalized NVIS "A" NVD input for each gray scale sample. Gray scale samples listed in Table 2 were measured under conditions of constant source irradiance. During the experiment, certain gray scale target samples receive more or less energy than others, due to uneven source irradiation, thus they will reflect more or less energy. Multiplication of the NVIS reflectance of each sample by the relative incident energy on each sample, yields the relative NVIS "A" energy reflected by each gray scale patch under the test conditions or, in other words, the NVD input relative to gray sample #1. This is displayed above in Table 4, Normalized NVIS "A" NVD Input. As in the previous table, all data is referenced to the center sample, #1. Column 1 shows the gray scale sample number, the second column depicts the normalized NVIS "A" reflectance from Table 2, column 3 contains the relative incident energy from Table 3 and column 4 contains the product of the two columns, the normalized NVD input.

TECHNICAL REPORT 95-003

GRAY SCALE SAMPLE #	NORMALIZED NVIS "A" REFLECTANCE RELATIVE TO SAMPLE #1 (Table 2)	RELATIVE INCIDENT ENERGY (Table 3)	NVIS "A" NVD INPUT NORMALIZED TO SAMPLE #1 (%)
1	1.000	1.000	100.00%
4	0.869	0.987	85.77%
8	0.729	0.994	72.46%
12	0.594	1.009	59.93%
16	0.446	1.019	45.45%
20	0.331	1.011	33.46%
24	0.201	0.980	19.70%
28	0.088	0.981	8.63%
30	0.036	0.965	3.47%

Table 4. Normalized NVIS "A" NVD Input

NVD BUNDLE OUTPUT COMPENSATION

As mentioned above, the monocular brightness varies across the fiber bundle output face. To determine the brightness variation, the irradiating source voltage was reduced to twenty volts, the laboratory lights secured, power to the NVD monocular applied, the NVD focused onto the wire

GRAY SCALE AREA SAMPLE #	AREA LUMINANCE (ft-L)	NORMALIZED UNCOMPENSATED NVD BUNDLE OUTPUT	RELATIVE INCIDENT ENERGY (Table 3)	NORMALIZED NVD BUNDLE OUTPUT
1	3.27 E-1 / 3.29	1.000	1.000	100.00%
4	2.79 E-1	0.851	0.987	86.22%
8	2.60 E-1	0.793	0.994	79.78%
12	2.89 E-1	0.881	1.009	87.31%
16	2.90 E-1	0.884	1.019	86.75%
20	3.16 E-1	0.963	1.011	95.25%
24	2.86 E-1	0.872	0.980	88.98%
28	2.89 E-1	0.881	0.981	89.81%
30	2.52 E-1	0.768	0.965	79.59%

Table 5. Normalized NVD Bundle Output Map

grid, and the photometer refocused onto the NVD fiber bundle output face. Photopic measurements in foot-Lamberts were made at the centroid of each of the nine squares defined by the wire grids that were visible on the fiber bundle output face. The raw bundle output data in foot-Lamberts are shown in Table 5, column 2. The same data are shown in column 3, after being normalized to the center

average. Sample locations are numbered as in the procedure above starting with #1 in the center, #4 at top center, #8 at top right, and so on. Two pieces of data are again recorded for sample location #1 and the average used as the normalized reference.

Unfortunately, the data shown in column 3 still contain an undesirable end product of uneven irradiance across the calibrated lambertian surface and luminance variation across the fiber bundle output. For this data to be useful, any artifacts caused by uneven target irradiance must be eliminated. By dividing each of the normalized target center referenced outputs in column 3 by the relative incident energy obtained from Table 3, it is possible to substantially remove the effects of uneven irradiation from the output data and obtain an independent NVD bundle output map. The end results are shown in Table 5, column 5.

NORMALIZED NVD OUTPUT

The following output data was collected with the gray scale target in place. As in the procedure described above, source voltage was adjusted, the laboratory lights secured, power to the NVD monocular applied, the NVD focused onto the gray scale target, and the photometer focused onto the NVD fiber bundle output face. Photopic measurements in foot-Lamberts were made at the centroid of each of the nine gray scale samples that were visible on the fiber bundle output face. Again, two pieces of data were collected for the center gray scale sample, #1.

Figures 10 through 13 are composites containing both experimental data and graphs. The data sets are organized from highest to lowest source voltage with two sets of data per figure. This grouping is purely for convenience and could in fact have been organized somewhat differently. Within each figure are two tables showing NVD input and output for two source voltage settings and a graph showing the two NVD responses.

Each table has six columns. From left to right they are: the gray scale sample numbers, the NVD NVIS input, the raw NVD output luminance data, the normalized center referenced NVD output, the bundle output compensation map, and finally the NVD output after compensation.

To justify the rationale for compensating the output data, it may be instructive to briefly revisit and describe Table 5, Normalized NVD Bundle Output Map. Table 5 is a map of the variance in luminance across the bundle output face normalized to the output at bundle center. Recall that each of the nine measured areas corresponds to a physical location on the bundle output face where a gray scale sample is displayed.

For the purposes of data comparison, any intrinsic reduction in luminance attributable to uneven bundle output can be offset by applying an equal but positive compensating gain. As an example, consider data presented for sample area #4 in Table 5. Data shown in column 5 indicates that under perfect conditions of even NVD photocathode illumination, the area of the bundle output face occupied by sample area #4 is nominally 0.8622 times as bright as that occupied by sample area #1. The gain required to compensate area #4, or, in other words, to cause the brightness of area #4 to be equal to that of area #1 is:

TECHNICAL REPORT 95-003

$$\text{Brightness area \#1} = (\text{Compensating Gain}) \times \text{Brightness area \#4}$$

or:

$$1.000 = (\text{Compensating Gain}) \times 0.8622$$

$$\text{Compensating Gain} = 1.000 \div 0.8622$$

$$\text{Compensating Gain} = 1.160$$

Therefore, any attenuation in luminance, attributable to the fiber bundle output and input optics of the NVD, in area #4 can be offset by applying a compensatory gain of 1.160 to any luminance data obtained in that position on the bundle output face.

Referring back to Figure 10, with a source voltage of 45 volts, the bundle output image of gray scale sample #4 has a luminance that is 0.7436 times that of gray scale sample #1. This difference in output luminance is a result of image gain as well as attenuation imposed by the optics and fiber optic bundle. Removal of unwanted attenuation effects requires a compensating gain. Experimental evidence indicates that compensation for the attenuation in this area requires a gain of 1.160 (or, $1 / 0.8622$). Multiplying the center referenced NVD output data in column 4 by the compensating gain for area #4 results in:

$$0.7436 \times 1 / 0.8622 = 0.8625$$

The product of this operation is shown in column 6 and is referred to as Compensated Center Referenced NVD Output. This is the gray scale sample's output value for the case of even target irradiance and no fiber bundle roll-off. Corresponding procedures have been applied to all the center referenced output data in Figures 11, 12 and 13.

For convenience, NVD response curves were generated in Figures 10 through 13 for each data set by plotting input data from column 2 versus output data from column 6. NVIS "A" radiance measurements are also supplied for purposes of comparison to night sky data.

OBSERVATIONS

By inspection, raw NVD output luminance data obtained with the irradiant source operating at an input voltage setting of 45 and at 40 volts in Figure 10 appear to be nearly identical. Indeed they should be since at this irradiant energy level, the NVD is operating in an automatic brightness control (ABC) mode (see Figure 2), and the averaged output over the whole fiber bundle output is fixed at a nominal value of 0.7 ft-L. Note that any one particular area of the output bundle may have a higher or lower luminance than the "nominal" average value depending upon the NVIS "A" reflectance of the gray scale sample that is imaged. In this particular instance the highest measured output is 4.72 ft-L and the lowest 0.17 ft-L. The graphed data clearly show a slight deviation from the expected linear response. Whether this is an indication of some inherent non-linearity in the NVD device, or an experimental artifact, is not known for certain.

Since the response curve seems to "peak" at gray scale sample #16, and since the physical location of sample #16 was at the center bottom, a good assumption is that the source irradiance was not evenly distributed across the target. Indeed, higher values for samples #20 and #12, located at

left and right bottom respectively, strongly indicate that our assumption of being able to define and map near-IR distribution by measurement of photopic distribution was in error. Our best guess is that the target bottom was irradiated by additional near-IR energy reflected from the optical bench. This "anomaly" is present to some extent in all the response curves.

A further comparison is made possible by the aid of the night sky energy data presented earlier in Table 1. The NVIS "A" radiance measured during that night at 2256 hours was 6.00×10^{-9} NR_A . This is reasonably close to the 6.11×10^{-9} NR_A value measured with the source voltage at 40 Volts. This indicates that if gray scale test target were positioned in the same plane as the lambertian surface used to gather the field data and had it been viewed by the NVD in the field as in the lab experiment, the NVD would have been operating in ABC mode. Further, the NVD output luminance of the gray scale samples would have been very close to that listed in column 3 of Figure 10.

When the source input voltage is operating at 35 volts or less, the radiant energy provided is not enough to drive the NVD into full ABC mode and the average bundle output is not clamped to 0.7 ft-L. Evidence for this can be seen by examining the raw output data in Figure 11 and noting that the highest output is 4.24 foot-Lamberts, or about 0.5 less than it was previously. At a source input voltage of 30 volts, the highest observed output is 2.43 foot-Lamberts, roughly 50 percent of what it was at 40 and 45 volts.

Under these input conditions, the graphed data show a similar response to that graphed previously with a slight "bump" in the curve. As before, the slight nonlinearity observed in the data could easily be attributable to experimental error.

Likewise, an analogous comparison can be made by noting the NVIS radiance measured in the field at 2100 hours, 3.62×10^{-9} NR_A and that measured in the lab with the source operating with an input voltage of 35 volts, 3.73×10^{-9} NR_A are within 3% of each other. Again, under similar field viewing conditions the NVD output luminance of the gray scale samples will be close to those obtained in the laboratory.

At source input voltages of 25 and 20 volts, the highest bundle outputs are 1.07 and 0.308 foot-Lamberts, respectively. Here, the data show more variability and non-linear behavior is either not present or is masked. The NVIS radiance measured with an input source voltage of 20 volts is about an order of magnitude less than the lowest NVIS radiance previously shown in Table 1.

Finally, at source input voltages of 15 and 10 volts the highest bundle outputs are 0.0457 and .0025 foot-Lamberts, respectively. The 15 volt NVD bundle output data are at levels that are roughly two decades less than equivalent data measured under ABC conditions. NVIS radiance is about 70 times less than the lowest NVIS radiance listed in Table 1.

Data taken with the source input voltage at 10 volts are highly irregular and strongly indicate that the equipment used to measure the NVD bundle output luminance was at the limit of its' ability to discriminate and measure small input power levels. Since our spectroradiometer was also at the limit of its' ability to measure, NVIS radiance is not shown.

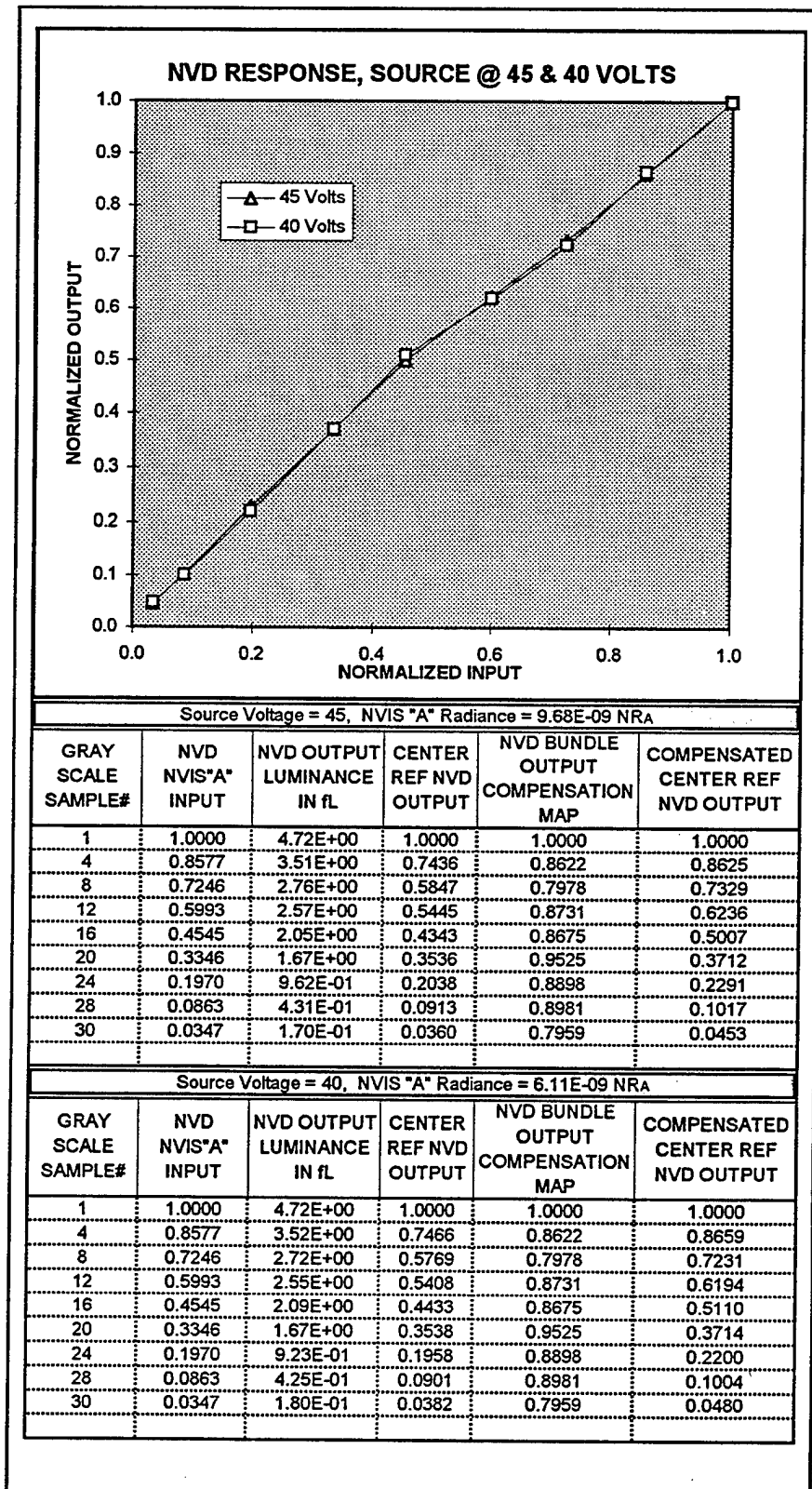


Figure 10. NVD Response, Source at 45 and 40 Volts

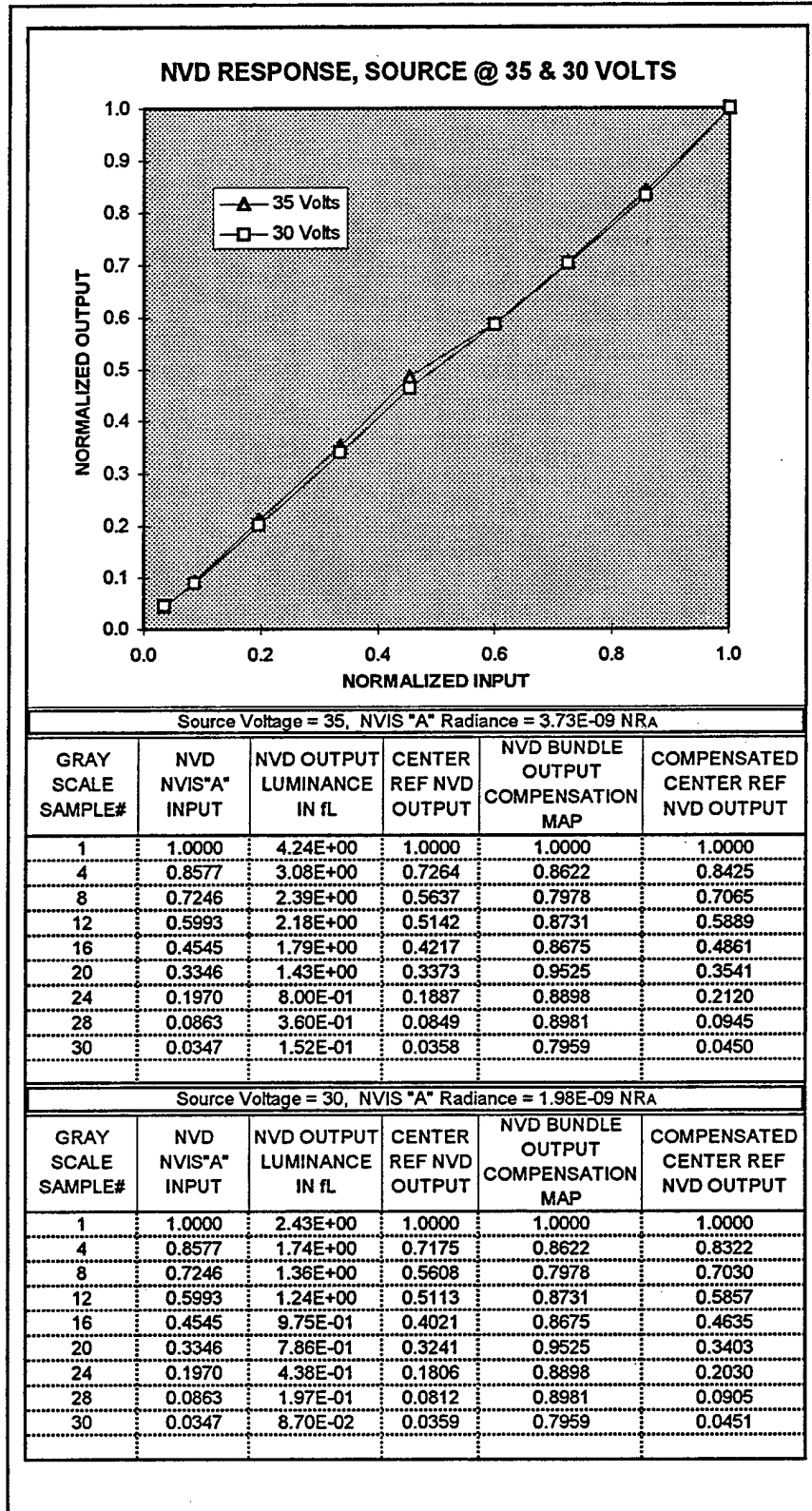


Figure 11. NVD Response, Source at 35 and 30 Volts

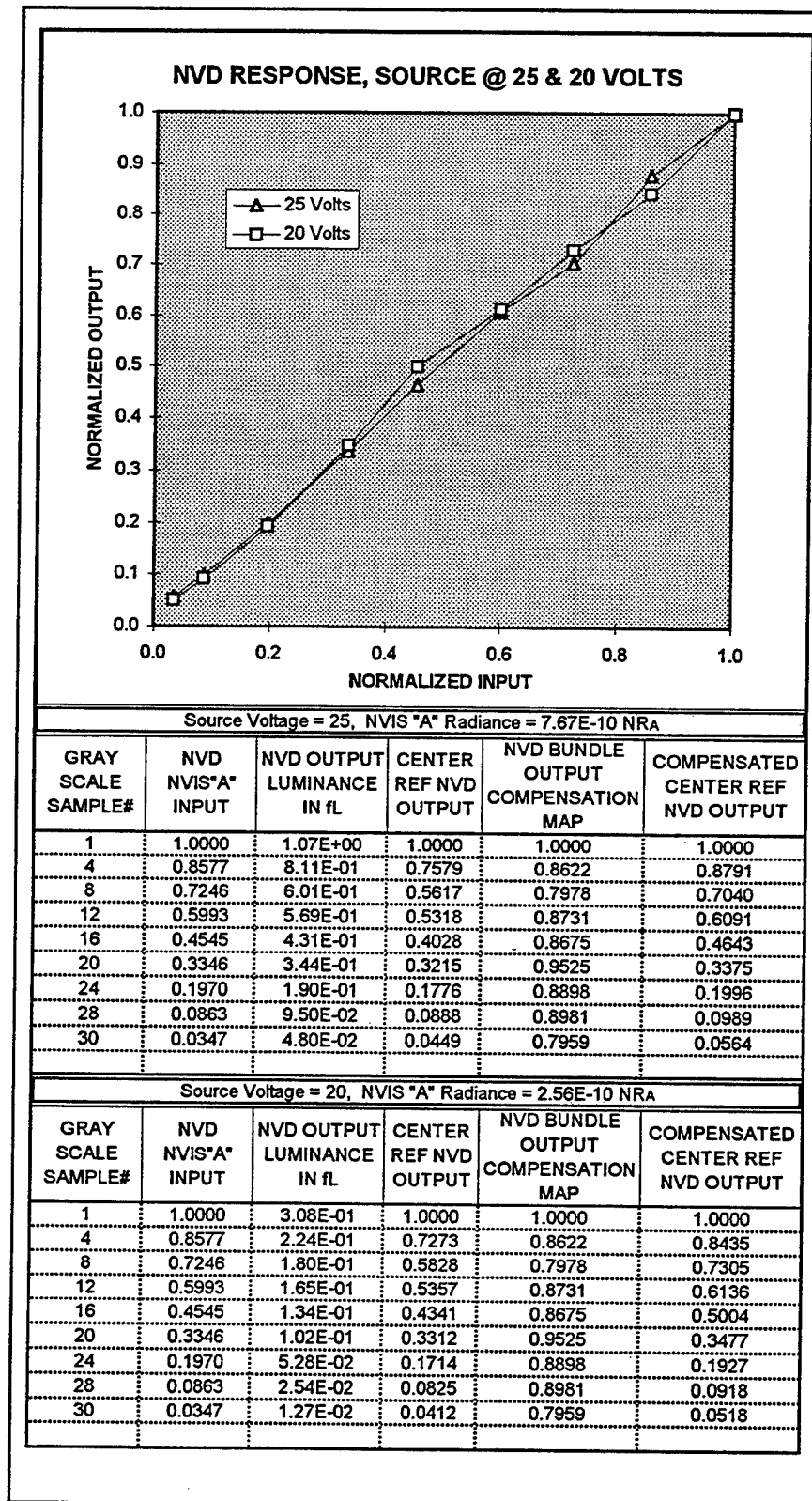


Figure 12. NVD Response, Source at 25 and 20 Volts

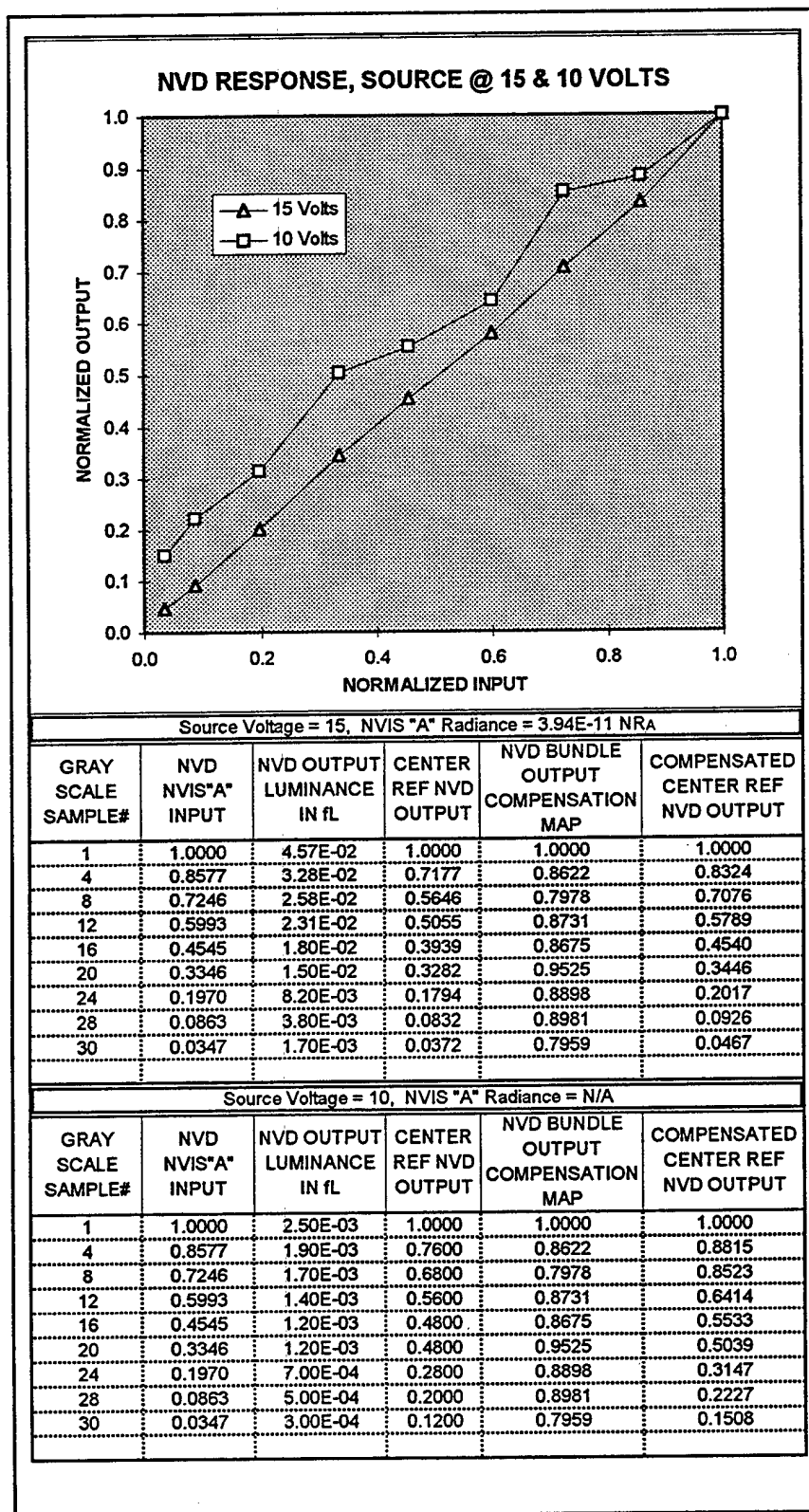


Figure 13. NVD Response, Source at 15 and 10 Volts

CONCLUSIONS

Within the ability of the instruments to measure and /or the abilities of the researchers, the data indicate that the imagery produced by this NVD monocular will have a gamma close to unity (1). For all practical purposes, our measurements and data indicate that this particular NVD is linear over a wide range of input levels.

Although an ANVIS was not used to obtain the data in this report, the observed gamma findings should be applicable since the NVD monocular used for data gathering has the same kind of image intensification tube and similar electronics. This does not imply that the operational characteristics of the two systems are identical, just that they are comparable. Since NVD output is dependent upon the intensification tube gain, the bundle output luminance range of another NVD monocular could be different at similar NVIS radiance inputs, but the image gamma will be close to one.

A linear ANVIS response leads to an interesting observation; the photopic contrast of two disparate objects (eg. the bahia grass and the sandy dirt road) measured at the output of the ANVIS will be identical to the NVIS contrast of the objects measured in a natural environment. The data show that this relationship holds true over a wide range of ambient night sky energy conditions. Changes in ambient night sky energy can alter the output luminance of the objects. But, the photopic contrast of the objects measured at the output of the ANVIS will remain constant.

These findings also reinforce the notion that the visibility of objects, even as viewed through the ANVIS, is still highly dependent upon the ability of human vision to discern between different luminances at low adapting luminance levels. As noted by Hood and Finkelstine (1986), classic laboratory studies by Blackwell (1946) and others indicate that under the best of conditions, the visual system can detect a difference in luminance (or contrast) of only about 1 percent. Further, contrast detection ability begins to decline for adapting luminance values less than 0.3 foot-Lamberts.

It is not known (by the authors) whether Blackwell's experimental results are directly, or even indirectly applicable, to ANVIS users, but if conditions are such that the average bundle output luminance is 0.3 foot-Lamberts, or less, it seems reasonable to assume that an observer's ability to detect objects with little contrast will be affected in some way. In cases of low ambient night sky irradiance, the ANVIS output luminance can be low enough to reduce the contrast detection ability of the observer to the point where the sandy dirt road disappears in the bahia grass field.

This suggests a possible strategy for simulation and training. All full night mission capable helicopter simulators now in use by the United States Navy and Marines Corps rely on NVD stimulation to provide the night vision imagery used by trainees. An image generator creates the simulated night environment imagery which is then viewed by operational NVDs. Practically speaking, all trainee knowledge of the near IR portion of the simulated night imagery is obtained through the NVD. It may be more effective to alter the gamma of the stimulating near IR imagery, rather than the average overall NVIS radiance, when simulating various (or varying) nighttime environmental conditions. Instead of allowing the NVD to be stimulated by less near IR energy, and

producing a lower NVD output, simulate the lower output of the NVD, and the human visual system's response to it, by altering the gamma of the stimulating near IR imagery.

Visibility of low contrast objects in the stimulating imagery is enhanced by lowering the gamma. Raising the gamma reduces the visibility. But the question is, can the gamma be changed to *correctly* simulate the visibility of these objects through an NVD under different environmental conditions? In order to be perceptually correct, one must understand and carefully consider the human visual system response to changes in NVD output luminance under the particular conditions being simulated. From a simulation and training standpoint, this approach might appear to have merit, but its validity and any subsequent improvements to training fidelity have yet to be determined.

THIS PAGE INTENTIONALLY LEFT BLANK

REFERENCES

Allen, J. H. & Hebb, R. C. (1993). Night Vision Camcorder System. (NAWCTSD Report No. 93-021). Orlando, FL: Naval Air Warfare Center, Training Systems Division

Hood, D. C. & Finkelstein, M. A. (1986). Sensitivity to Light. Chapter 5 of Handbook of Perception and Human Performance edited by K.R. Boff, L. Kaufman & J.P. Thomas, New York: Wiley & Sons

Image Intensifier Assembly, 18MM, Microchannel Wafer MX-10160/AVS-6, MILSPEC MIL-I-49428(CR). (1989). Military Specifications

Lighting, Aircraft, Interior, Night Vision Imaging System (NVIS) Compatible, MILSPEC MIL-L-85762A(CR). (1988). Military Specifications

Stephanik, R. J. (1989). Night Sky Radiometric Measurements During Follow-On-Evaluation Testing of AN/PVS-7 (A,B) At Fort Benning, GA. (CNVEO Report No. AMSEL-NV-TR-0079). Fort Belvoir, VA: Center for Night Vision and Electro-Optics

THIS PAGE INTENTIONALLY LEFT BLANK

TECHNICAL REPORT 95-003

DISTRIBUTION LIST

Defense Technical Information Center 2 Copies
8725 John J. Kingman Road, Suite 0944
Ft Belvoir, VA 22060-6218

Office of Naval Research
Code 342, ATTN: Dr. Stan Collyer
800 North Quincy Street
Arlington, VA 22217-5000

Research and Engineering Competency
Training Systems Department
Naval Air Warfare Center
TSD 4.9
12350 Research Parkway
Orlando, FL 32826-3224

Program Directorate
Naval Air Warfare Center
Training Systems Division
TSD 4.9T
12350 Research Parkway
Orlando, FL 32826-3224

Research and Engineering Competency
Science and Technology Division
Naval Air Warfare Center
Training Systems Division
TSD 4.9.6
12350 Research Parkway
Orlando, FL 32826-3224

Armstrong Labs/Aircrew Training Research
ATTN: Dr. Elizabeth Martin
6001 S. Power Road, Bldg 558
Mesa, AZ 85206-0904

TECHNICAL REPORT 95-003

THIS PAGE INTENTIONALLY LEFT BLANK